Oxidative stress and inflammatory response of AgNPs and chitosan-coated AgNPs (25nm) via different doses in mice

Samar M Gooda
National Research Center
Eman M Abd El-Azeem
Ain-Shams University
Nagy S El-Rigal
National Research Center
Sanaa A Ali (sanaa_ahmedibrahim@yahoo.com)
National Research Center
Wagdy KB Khalil
National Research Center
Amina M Medhat
Ain-Shams University

Research Article

Keywords: AgNPs, Chitosan, Liver, Oxidative stress, DNA damage

Posted Date: March 30th, 2022

DOI: https://doi.org/10.21203/rs.3.rs-1425133/v1

Abstract

Objective

The cytotoxicity of AgNPs in mice comparatively with chitosan-coated AgNPs. Silver and chitosan–coated AgNPs of average size 25 ± 5 nm, which were prepared and characterized at Nanotech Egypt for Photo-Electronics

Methods

Male mice were administered with different doses of 25, 50, and 100 mg/kg of both nanoparticles, oxidative stress markers; liver functions, pro-inflammatory cytokines and some tumor markers were measured

Results

AgNPs significantly increased malondialdehyde and nitric oxide levels. Moreover, it was found that AgNPs significantly increased the levels TNF-α and IL-6 as well as the levels of α-L-fucosidase and arginase and DNA damage measured by comet assay. On the contrary significantly decreased superoxide dismutase and reduced glutathione levels. They also led to deteriorations in serum aminotransferases, alkaline phosphatase and γ-glutamyltransferase levels, chitosan–coated AgNPs reduced the inflammatory caused in hepatic cells.

Conclusion

Chitosan–coated AgNPs was decreased AgNPs toxicity, by improving the biochemical parameters enrolled in this study, chitosan–coated AgNPs had less cytotoxic effects on liver function, and inflammatory biomarkers.

Introduction

An exponential increase in the applications of nanomaterials in medical and healthcare products has been reported in recent years due to their unique physical and chemical properties. The human exposure to these products is rapidly increasing and, therefore, their potential for adverse health effects is of concern. Silver nanoparticles (AgNPs) are one of the most widely used nanoparticles in commercial products owing to their unique and attractive antibacterial, antiviral and antifungal effects [1, 2].

Silver nanoparticles and their composites have been broadly applied in medical and consumer products, such as disinfectants for medical devices, food packaging and clothing. Additionally, their special optical properties allow AgNPs to be incorporated into biological and chemical sensors [3, 4].

In vivo bio-distribution and toxicity studies clarified that dietary AgNPs reduced the growth rate of the exposed mice and rats and affected the intestinal microvilli and the liver [5].

The possible mechanism for AgNPs cytotoxicity is free radical generation, particularly reactive oxygen species (ROS) and reactive nitrogen species (RNS) formation in various cells that lead to oxidative stress [6].

Numerous methods for the synthesis of AgNPs have been developed such as chemical reduction of silver salt solution using reducing agents. However, most reducing agents lead to environmental toxicity or biological hazards. In addition, different stabilizers, such as citrate or polyvinylpyrrolidone (PVP) are used to control the size of silver and the release of silver into the surrounding media. Therefore, the biological synthesis of AgNPs became the future trend-using polymer matrices, which are non-toxic, can be easily designed into almost any shape required for a particular application and act as both a stabilizing and a reducing agent such as starch, chitosan and cyclodextrins [7].

A nontoxic stabilizing or capping agent should be selected during the synthesis of nanoparticles because the toxicity of the nanoparticles depends on the properties of the capping agent rather than the nanoparticle itself [7].

Chitosan is the N-deacetylated derivative of chitin, a natural polymer found in the shells of crustaceans and is structurally similar to hyaluronic acid (extracellular matrix). The positive charge of chitosan affords the polymer numerous and unique physiological and biological properties [8]. The excellent properties of chitosan, including its biocompatibility, bioactivity, low cost and nontoxic byproducts make it easy to functionalize for biomedical applications [9].

Therefore, this study was constructed to evaluate the cytotoxicity of silver nanoparticles in mice comparatively with chitosan-coated silver nanoparticles with the same size at different doses on liver enzymes, some oxidative stress markers and tumor markers and DNA damage degree.

Materials And Methods

Chemicals

All chemicals used in the present study were high analytical grade products and purchased from Sigma (USA), Merck (Germany), Riedel de Hàen (Germany), BDH (England) and Fluka (Switzerland). Kits used for the quantitative determination of different parameters were also purchased from Quimica Clinica Aplicada (QCA) (Spain), and Biodiagnostic.

Preparation of Nanoparticles

Nanoparticles were prepared at Nanotech Egypt for Photo-Electronics as follows:

Silver nanoparticles has been prepared by a chemical reduction method as reported by [10]. A solution of $AgNO_3$ has been used as (Ag^+) ions precursor, sodium borohydride ($NaBH_4$) as reducing agent and polyvinyl pyrrolidone (PVP, Av. Wt 30,000 – 40,000) as stabilizing agent. Ten mL of 1 mM $AgNO_3$ with 1 g of PVP were brought to reflux during stirring, and then 2 mL

of 1 mM ice cooled NaBH4 solution were added drop wise under vigorous stirring to prevent further growth and aggregation. The color of the solution slowly turned into grayish yellow, indicating the reduction of the (Ag^+) ions to Ag nanoparticles. The solution was left for 15 min at room temperature to obtain uniform mixing and good size distribution.

Chitosan-coated silver nanoparticles were prepared according to [11, 12]. Blank nanoparticles were obtained upon the addition of a tripolyphosphate (TPP) aqueous solution to a chitosan solution, then silver-chitosan Nano-hybrids has been obtained via *in-situ* reduction of silver ions (Ag^+) using the amine and OH functional groups existing on the Chitosan molecules.

Characterization– Size & Shape

Transmission electron microscope (TEM) was performed using JEOL JEM-2100 high-resolution transmission electron microscope (HRTEM) at an accelerating voltage 200 kV.

Optical Properties: Ultra violet- Visible (UV-Vis) absorption spectra were obtained on an Ocean Optics USB2000 + VIS-NIR Fiber optics spectrophotometer.

Animals

Fifty-six Male Swiss albino mice (30–35 g) were obtained from the animal house of National Research Center (Dokki, Giza, Egypt) and were allowed free access to standard diet and water all over the period of the experiment.

Experimental design

After an acclimatization period of 1 week, animals were divided into seven groups (8 mice/ group) and housed individually in filter top polycarbonate cages. According to the LD_{50} dose of Ag NPs (~2 g/kg b.wt.) Ohkawa [13], three doses of Ag and chitosan-coated silver NPs, 25, 50, and 100 mg/kg b.wt (i.e., 0.0125, 0.025, and 0.05 LD_{50}) were applied.

Group 1: Normal control mice. Group 2–4: Mice orally administered daily for 14 days with doses of 25, 50 and 100 mg/ kg body weight with silver nanoparticles (size: 25 ± 5 nm).Group 5–7: Mice orally administered daily for 14 days with doses of 25, 50 and 100 mg/ kg body weight with chitosan-coated silver nanoparticles (size: 25 ± 5 nm).

Handling, anesthetic and sacrifice procedures were approved by the medical research ethics committee of the National Research Centre in Egypt with registration **No. 13 087** according to the guidelines of the Ethical Committee of the Federal Legislation and National Institutes of Health Guidelines in USA.

Tissue homogenates

Liver tissues were homogenized in 0.9 M NaCl. Homogenate was centrifuged at 3,000 rpm at 4^{o}C for 5 minutes and the supernatant was stored at -20°C for different biochemical assays.

Serum sample

The sub-tongual vein was punctured in each animal; blood was collected, left to clot, and then centrifuged at 3,000 rpm for serum separation. The separated serum was stored at -80^{o}C.

Biochemical Parameters

Total protein was estimated calorimetrically according to [14].

Oxidative Stress Markers

Estimation of lipid peroxides - Lipid peroxide was determined as malondialdehyde. Its concentration was calculated using the extinction coefficient value $1.56 < 10^{5}\ M^{-1}\ cm^{-1}$ and read at 540 nm in spectrophotometer [15].

Estimation of Nitric oxide - Nitric oxide was determined in tissue liver homogenate. The assay

is based on the enzymatic conversion of nitrate to nitrite by nitrate reductase. The reaction is followed by colorimetric detection of nitrite as an azo dye product of the Giess Reaction which can be measured colorimetrically at wavelength 540 nm [16].

Estimation of glutathione - Glutathione was estimated using sodium phosphate buffer and 2 mM dithiobisnitrobenzoic acid (DTNB). The developed color was read at 405 nm within 5 min in spectrophotometer. The amount of glutathione was calculated from a standard curve plotted for serial concentrations of glutathione (5–100 µg) [17].

Estimation of superoxide dismutase enzyme - Catalase activity was assayed spectrophotometrically following decrease in absorbance at 560 nm. This assay relies on the ability of the enzyme to inhibit the phenazine methosulphate-mediated reduction of nitroblue tetrazolium dye [18].

Serum Liver Enzymes

Estimation of aminotransferases - AST and ALT were measured using the QCA Diagnostic kits (Spain). The colorimetric determination of AST and ALT depends on determining amounts of the coloured hydrazones formed from the 2, 4-dinitrophenylhydrazine of oxaloacetate and pyruvate, the color of which is read at 505 nm [19].

Estimation of alkaline phosphatase - Enzyme was estimated using QCA Diagnostic kits (Spain) as a colourless substrate of phenolphthalein monophosphate, hydrolysed by alkaline phosphatase giving rise

to phosphoric acid and phenolphthalein which, at pH values, turns into a pink colour that can be photometrically determined at 550 nm [20].

Estimation of γ-glutamyltransferase (γ-GT) - was determined according to the kinetic method using QCA Laboratory Diagnostic kits (Spain) [21].

Tumor Markers

Determination of α-L-fucosidase level - This was done using Diagnostic kits as the enzymatic cleavage of the synthetic substrate p-nitrophenyl- α-L-fucopyranoside to p-nitrophenol and L-fucose produced yellow color in an alkaline medium which can be measured quantitatively at 404 nm [22].

Determination of arginase level - This assay by Biodiagnostic is based upon the colorimetric determination of urea at 525 nm by condensation with diacetyl monoxime in an acid medium in the presence of ferric chloride (oxidant) and carbazide (accelerator) [23].

Anti-inflammatory Markers

Estimation of tumor necrosis factor-α (TNF-α) - Liver TNF-α level was measured by a quantitative enzyme-linked immunosorbent assay (ELISA) technique according to the manufacturer's instructions using the Quantikine TNF-α Immunoassay kit (R&D systems, USA) [24].

An aliquot of sample or calibrator containing the antigen to be quantified is allowed to bind with a solid phase antibody. After washing, enzyme labeled antibody is added to form a sandwich complex of solid phase Ab-Ag-Ab enzyme. Excess (unbound) antibody is then washed away, then enzyme substrate is added. The enzyme catalytically converts the substrate to product, the amount of which is proportional to the quantity of antigen in the sample.

Estimation of interleukin-6 (IL-6) - Liver IL-6 level was measured by a quantitative enzyme –linked immunosorbent assay (ELISA) technique according to the manufacturer's instructions using the Quantikine IL-6 Immunoassay kit [25].

Comet Assay

Isolated liver tissues of all groups of mice were subjected to comet assay. About 500 cells per animal were randomly selected from each sample and the comet tail DNA was analyzed with DNA damage analysis software (Comet Score, TriTek corp., Sumerduck, VA22742). Endogenous DNA damage was measured as the mean comet tail DNA of liver tissues of several groups [26, 27].

Histological studies

Liver slices were fixed in 10% paraformaldehyde and embedded in paraffin wax blocks, stained with hematoxylin & eosin (H&E), then examined under light microscope for determination of histological changes [28].

Statistical analysis

All data were expressed as mean ± SD. Statistical analysis was carried out by one-way analysis of variance (ANOVA) using SPSS 12 (Statistical Package for the Social Science; SPSS Inc., Chicago, IL, USA) Computer Program followed by Turkey's multiple comparisons post hoc test (LSD) (Least significant difference) using CoStat Computer programme (CoHort Software, version 6.303, Monterey, USA), where unshared superscript letters indicate that these groups are significantly correlated at $P \leq 0.05$.

Results

Characterization of nanoparticles

The quality of the prepared nanoparticles was ensured by measuring their optical properties and determining their particle size and shape using HRTEM.

The prepared AgNPs and chitosan-coated silver nanoparticles were isolated to different particle sizes by size fractionation process by centrifugation at different times and speeds. Visual observation of the separated nanoparticles showed that AgNPs with 25 ± 5 nm particle size are yellow, whereas chitosan-coated silver nanoparticles with the same size showed brown color.

The UV–Vis absorption spectrum illustrated in Fig. 1 showed a well-defined absorption peaks for the 25 ± 5 nm particle size. This corresponds to the wavelength of the surface plasmon resonance (SPR) of AgNPs. This particle size showed the maximum SPR peak (black line) as a sharp absorption band at λmax = 401 nm for AgNPs and an absorption band (red line) with a maximum at λmax = 425 ± 5 nm for chitosan-coated silver nanoparticles.

The TEM images of nanoparticles were represented in Fig. 2 (A, B). Both samples showed mainly spherical, mono dispersed nanoparticles without any agglomeration. The average particle size for both particles was 25 ± 5 nm according to image processing and analysis program (Image J).

Biochemical Investigations

Data represented in Table 1 showed a significant increase in MDA and NO levels after oral administration of AgNPs (25 ± 5 nm) in almost all doses. In contrast, there was a significant decrease in levels of GSH and SOD compared to normal mice. Meanwhile, data in Table 1revealed that oral administration of chitosan-coated AgNPs (25 ± 5 nm) at all doses significantly improved the deterioration in the levels of MDA and NO compared to AgNPs administrated groups. In addition, chitosan-coated AgNPs administration restored the levels of GSH and SOD in almost all doses when compared to control group.

Table 1
Descriptive analysis of AgNPs and chitosan-coated AgNPs 25 ± 5 nm on the levels of some biochemical parameters in studied groups

Groups	Control	Ag Nps (25 ± 5 nm)			Ch-Ag Nps (25 ± 5 nm)		
Parameters		25 mg/kg	50 mg/kg	100 mg/kg	25 mg/kg	50 mg/kg	100 mg/kg
MDA (nmole /mg protein)	6.4 ± 0.39^{e}	10.12 ± 0.92^{d,e}	14.82 ± 2.41^{b}	17.51 ± 2.5^{a}	7.50 ± 0.25^{f}	10.43 ± 0.66^{d,e}	12.49 ± 0.72^{c}
NO (µmole/g tissue)	10.33 ± 0.47^{e}	13.66 ± 1.23^{d}	18.13 ± 2.82^{b}	20.74 ± 2.72^{a}	11.02 ± 0.42^{e}	13.49 ± 0.58^{d}	15.85 ± 0.96^{c}
GSH (µg/mg protein)	76.92 ± 5.3^{a}	75.86 ± 4.13^{b,c}	48.32 ± 2.26^{e}	40.98 ± 1.55^{f}	57.74 ± 3.24^{b}	55.18 ± 1.91^{e}	48.41 ± 3.92^{f}
SOD (U/mg protein)	25.05 ± 0.71^{a}	19.57 ± 1.4^{c,d}	16.3 ± 2.19^{e}	14.1 ± 1.73^{f}	22.55 ± 1.04^{b}	18.09 ± 0.87^{d}	15.31 ± 0.93^{e,f}
s-AST (U/ml)	41.66 ± 4.89^{g}	51.71 ± 1.74^{d}	59.52 ± 2.23^{b}	63.62 ± 1.86^{a}	48.41 ± 1.06^{e}	52.92 ± 1.56^{c,d}	58.29 ± 2.43^{b}
s-ALT (U/ml)	20.22 ± 2.22^{d,e}	23.58 ± 1.59^{c}	28.84 ± 1.18^{b}	34.17 ± 2.33^{a}	21.42 ± 0.92^{d}	25.64 ± 0.81^{c}	28.24 ± 1.78^{b}
-GT (U/mg protein)	31.22 ± 4.17^{a}	12.81 ± 1.24^{d,e,f}	9.49 ± 1.26^{g}	8.43 ± 1.44^{g}	17.56 ± 1.24^{b}	14.12 ± 0.79^{c,d,e,f}	14.44 ± 1.24^{c,d,e,f}

 Data are expressed as means ± SD.

 AgNps: silver nanoparticles, Ch-AgNps: chitosan-coated silver nanoparticles.

 MDA: Malondialdehyde, NO: Nitric Oxide, GSH: Reduced-Glutathione, SOD: Super-oxide Dismutase

 AgNps and Ch-AgNPs of average size 25 ± 5 nm were administered orally to fifty-six male Swiss Albino mice divided into six groups, with a dose of 25, 50, and 100 mg/kg of both nanoparticles, in addition to a control group.

 Analysis of data is carried out by one way (ANOVA) (analysis of variance) accompanied by post hoc (LSD) (Least significant difference) (CoStat Computer programme).

 Unshared letters indicate significance correlation at $P \leq 0.05$.

Groups	Control	Ag Nps (25 ± 5 nm)			Ch-Ag Nps (25 ± 5 nm)		
Parameters		25 mg/kg	50 mg/kg	100 mg/kg	25 mg/kg	50 mg/kg	100 mg/kg
ALP (U/L)	6.33 ± 0.84^{f}	10.92 ± 0.93^{e}	17.35 ± 2.86^{a,b}	19.09 ± 3.33^{a}	8.63 ± 0.31^{e}	10.94 ± 0.73^{e}	14.51 ± 0.85^{c,d}
□ Data are expressed as means ± SD.							
□ AgNps: silver nanoparticles, Ch-AgNps: chitosan-coated silver nanoparticles.							
□ MDA: Malondialdehyde, NO: Nitric Oxide, GSH: Reduced-Glutathione, SOD: Super-oxide Dismutase							
□ AgNps and Ch-AgNPs of average size 25 ± 5 nm were administered orally to fifty-six male Swiss Albino mice divided into six groups, with a dose of 25, 50, and 100 mg/kg of both nanoparticles, in addition to a control group.							
□ Analysis of data is carried out by one way (ANOVA) (analysis of variance) accompanied by post hoc (LSD) (Least significant difference) (CoStat Computer programme).							
□ Unshared letters indicate significance correlation at $P \leq 0.05$.							

In addition, significant elevations in levels of s-AST, s-ALT and ALP and a significant depletion in γ-GT were observed after oral administration of AgNPs (25 ± 5 nm) compared to the control group.

However, amelioration in these enzymes levels were observed after oral administration of chitosan-coated AgNPs with respect to AgNPs administrated groups with varied significances.

Results in Table 2revealed a significant increase in the levels of serum α-L-fucosidase and arginase compared to control group, whereas improvement in their levels was observed after oral administration of chitosan-coated AgNPs (25 ± 5 nm) with respect to AgNPs administrated groups.

Table 2
Descriptive analysis of AgNPs and chitosan-coated AgNPs 25 ± 5 nm on the levels of some tumor and anti-inflammatory markers in studied groups

Groups	Control	Ag Nps 25 ± 5 nm			Ch-Ag Nps 25 ± 5 nm		
Parameters	(G1)	25 mg/kg (G2)	50 mg/kg (G3)	100 mg/kg (G4)	25 mg/kg (G5)	50 mg/kg (G6)	100 mg/kg (G7)
α-L-fucosidase (U/L)	2.73 ± 0.43^{f}	4.87 ± 0.68^{b,c,d}	5.67 ± 0.62^{a,b}	6.15 ± 0.62^{a}	3.73 ± 0.64^{e}	4.96 ± 0.51^{b,c,d}	5.08 ± 0.53^{b,c,d}
Arginase (U/L)	91.74 ± 12.06^{h}	130.68 ± 7.24^{d,e}	143.75 ± 6.39^{b,c}	158.38 ± 7.72^{a}	127.02 ± 3.99^{e}	137.74 ± 4.39^{c,d}	133.29 ± 5.45^{d,e}
TNF-α (pg/mL)	17.38 ± 0.91^{h}	27.09 ± 1.58^{e}	32.45 ± 0.90^{c}	41.66 ± 0.82^{a}	25.3 ± 0.82^{f}	26.16 ± 0.43^{e,f}	34.66 ± 0.94^{b}
IL-6 (pg/mL)	15.55 ± 0.52^{j}	35.19 ± 1.05^{f}	41.89 ± 0.81^{b}	44.91 ± 1.23^{a}	30.64 ± 1.07^{h}	38.56 ± 0.45^{d}	41.45 ± 1.33^{b}

 Data are expressed as means ± SD.

 AgNps: silver nanoparticles, Ch-AgNps: chitosan-coated silver nanoparticles.

 α-L-fucosidase and Arginase are tumor markers, TNF-α: Tumor necrosis factor- α, IL-6: Interleukin-6

 AgNps and Ch-AgNPs of average size 25 ± 5 nm were administered orally to fifty-six male Swiss Albino mice divided into six groups, with a dose of 25, 50, and 100 mg/kg of both nanoparticles, in addition to a control group.

 Analysis of data is carried out by one way (ANOVA) (analysis of variance) accompanied by post hoc (LSD) (Least significant difference) (CoStat Computer programme).

 Unshared letters indicate significance correlation at $P \leq 0.05$

Meanwhile, oral administration of AgNPs with different doses demonstrated a significant increase in the levels of TNF-α and IL-6 compared to control group and chitosan-coated AgNPs (25 ± 5 nm) oral administration significantly retrieved their levels for almost all doses.

Table 3showed the oxidative DNA damage in the liver cells of mice evaluated by the Fpg-modified Comet assay after exposure to AgNPs and chitosan- coated AgNPs (25 ± 5) with doses 25, 50 and 150 mg/kg. Comet assay showed that DNA damage levels were significantly increased with various values recording the highest damage (23.4%) with AgNPs 25 ± 5 nm and dose 100mg/kg.

Table 3
Visual score of DNA damage in liver tissues from different treated groups (Comet Assay)

Treatment		No. of cells		Class**				% of cells with DNA damage
		Cell Analyzed*	No of comets	0	1	2	3	
Control		500	33	467	26	7	0	6.6
Ag NPs 25 ± 5 nm	25 mg/kg	500	49	451	25	16	8	9.8
	50 mg/kg	500	89	411	29	33	27	17.8
	100 mg/kg	500	117	383	27	39	51	23.4
Ch-Ag NPs 25 ± 5 nm	25 mg/kg	500	46	454	22	19	5	9.2
	50 mg/kg	500	58	442	19	24	15	11.6
	100 mg/kg	500	61	439	22	21	18	12.2

*: Number of cells examined per group, **: Class 0 = no tail; 1 = tail length < diameter of nucleus; 2 = tail length between 1X and 2X the diameter of nucleus; and 3 = tail length > 2X the diameter of nucleus.

 AgNps: silver nanoparticles, Ch-AgNps: chitosan-coated silver nanoparticles.

 AgNps and Ch-AgNPs of average size 25 ± 5 nm were administered orally to fifty-six male Swiss Albino mice divided into six groups, with a dose of 25, 50, and 100 mg/kg of both nanoparticles, in addition to a control group.

In addition, class 2 of DNA damage was estimated in this group and revealed 33.3% compared to only 21.2% in normal cases. Moreover, class 3 of DNA damage that is considered the highest damage of DNA occurred only in AgNPs 25 ± 5 nm and dose 100mg/kg (43.6%) and was not present in controls as shown in Figure (3).

Figure (4), showed the histological examination of liver sections after oral administration of AgNPs (25 ± 5 nm) with different doses, where focal areas of inflammatory cells aggregation, focal necrobiosis in the hepatic parenchyma Fig. 4(B), periductal inflammatory cells infiltration surrounding the bile duct Fig. 4 (C) and cloudy swelling as well as hydropic degeneration of hepatocytes were seen in some parts; showing degenerative changes in the hepatocytes surrounding and adjacent the dilated central vein Fig. 4 (D).

While, liver sections of mice administered with chitosan-coated AgNPs (25 ± 5) in figure (4) showed noticeable degrees of improvements in comparison to AgNPs administrated groups represented by decrease in periductal inflammatory cells infiltration surrounding the bile ducts Figure 4 (E and F), in addition to fewer degrees in degeneration detected in the hepatocytes adjacent and surrounding the dilated central vein Fig. 4 (G).

Discussion

Currently, silver nanoparticles are one of the most widely used NPs in commercial products because of their strong anti-inflammatory and antimicrobial properties [1]. The small size of nanoparticles defines their distinct target organs and bio-distribution pattern. The impact of particle size to the AgNPs toxicity on cell death and cell cycle progression has been reported [29, 30]. Particle size plays an important role on the uptake kinetics of NPs in the cells [31, 32].

In line with previous published data, the current study has demonstrated that AgNPs (25 ± 5 nm) administration to mice induced oxidative stress in their liver tissues indicated by significant elevation in MDA with concomitant increase in NO level in liver in comparison to control mice, accompanied with significant depletion in the other antioxidant parameters; GSH and SOD.

AgNPs have the ability to generate ROS/RNS that lead to oxidative stress and tissue damage. These ROS and RNS can initiate lipid peroxidation, result in DNA strand breaks, and indiscriminately oxidize all molecules in biological membranes and tissues resulting in increase in levels of MDA [33, 34].

Nitric oxide is an ambivalent agent that behaves as a mediator of inflammation and as a regulator of redox metabolism. The exposure to different AgNPs doses caused an increase of nitric oxide levels, which can be associated with either cell activation or cytochrome C release from mitochondria and apoptosis [34].

The antioxidants GSH and SOD can quench free radicals or serve as a substrate for other antioxidant enzymes, such as glutathione peroxidase and glutathione reductase [35].

The decreased levels of GSH and SOD after exposure to AgNPs and their toxic effect on the mitochondria of liver, may be due to complexing of AgNPs with thiol groups, leading to production of ROS and oxidative stress[34, 36], or to increasing use of GSH to downplay the effect of free radicals after exposure to the nanoparticles [37].

In this study, administration of chitosan-coated AgNPs greatly improved the level of the hepatic oxidative stress markers MDA and NO meanwhile up regulating the levels of the antioxidant markers GSH and SOD compared to their corresponding groups of AgNPs with varied significances.

This improvement may be attributed to the properties of chitosan, including its biocompatibility, bioactivity and biodegradability. In addition, the antioxidant activity of chitosan can be attributed to *in vitro* and *in vivo* free radical-scavenging activities [38].

In the present study, intoxication with AgNPs caused damage of liver and lead to increase in the activities of serum AST, ALT and ALP and a decrease in γ-GT enzyme level indicating a destruction of hepatocytes architecture because of oxidative stress relative to size and composition of these particles in agreement with [39].

The increase in AST and ALT after nanosilver exposure was in accordance with the histological findings. Hence, the increase of these enzymes is an indicator of liver damage and thus otherwise alterations in the hepatic function [40].

The decline observed in γ-GT enzyme is an indication of impaired GSH synthesis. In addition, γ-GT enzyme is the first enzyme in the degradation of GSH to its precursor amino acids making them available for reuptake and reutilization by the cell for GSH resynthesis [41].

Meanwhile, ALP enzyme elevation in serum is correlated with the presence of bone, liver, and other diseases [42], which may be attributed to the proliferation of bile ductules and bile canaliculi as a result of nanoparticles exposure or due to increased loss of intracellular enzyme by

diffusion through cell membranes which appears to act as a stimulus to the synthesis of more enzyme protein in agreement with [32, 43]

On the other hand, administration of chitosan-coated AgNPs to mice significantly restore AST, ALT, γ-GT and ALP activities compared to AgNPs administrated groups with varied significances. This may indicate that coating with chitosan tend to attenuate liver damage by maintaining the integrity of the plasma membranes, thereby suppressing the leakage of enzymes through membranes, exhibiting hepatoprotective activity.

The present data showed that AgNPs induced a significant elevation in α-L-fucosidase and arginase activities compared to control mice. The elevation of tumor markers and their release in the sera may result from the liver abnormalities and toxicity induced by AgNPs that leads to accumulation of glutamate or other alterations in enzymes of the glutamate-GABA (glutamate and alpha-amino butyrate) system [44].

The inhibitory effect of chitosan-coated silver nanoparticles on the activity of these tumor markers may indicate the significant antitumor activity of chitosan due to its non-toxic, biocompatible and bioactive properties. The antitumor mechanism of chitosan nanoparticles was related to its membrane-disrupting and apoptosis-inducing activities [45].

Nanoparticles are also known to up-regulate the transcription of various pro-inflammatory genes due to oxidative stress, including TNF-α, IL-1, IL-6 and IL-8, by activating nuclear factor-kappa B (NF-κB) signaling [46].

In this regard, the present data showed that AgNPs induced a significant elevation in TNF-α and IL-6 levels demonstrating the most inflammatory potential of AgNPs at the higher doses that can be an

important sign of NP toxicity [38, 47], while chitosan-coated silver nanoparticles significantly attenuated these elevated levels, indicating that the anti-inflammatory role of this coating is associated with the oxidative damage.

Results of the current study were confirmed by studying the degree of DNA damage after AgNPs as an evidence for the stress. Comet assay showed that DNA damage, which appear like comets, increased significantly in all AgNPs administered groups compared to that of the control group. The increasing in DNA damage observed a clear induction in DNA breaks [48, 49]. However, DNA damage, appearing like comets is significantly restored in animals administered chitosan-coated silver Nano composites as a further indication of anti-apoptotic activity and significant tumor regression of chitosan coating in agreement with [50].

There is evidence that histological changes in liver tissue following AgNPs exposure may be associated with oxidative stress [51]. The connection between AgNPs, behavioral changes, oxidative stress, apoptosis and histopathological modification could be ROS as the key molecules [52, 53]. Microscopic study of liver revealed that various alterations denoting the hepatotoxic effect of AgNPs including hepatocellular degeneration and focal necrobiosis in the hepatic parenchyma were the most recognized hepatic changes that were dose dependent.

Administration of chitosan-coated silver nanoparticles showed marked reduction in

histological structure of the liver compared to AgNPs administered groups. These were paralleled with the results of biochemical analysis of the present study [54].

Conclusion And Recommendations

The liver enzymes, oxidative stress markers, DNA damage degree and liver histological pattern were greatly influenced in a dose dependent manner by AgNPs (25 ± 5 nm) causing profound toxic effects. Chitosan-coated AgNPs administration reduced the toxic effect of AgNPs, for this we have noticed restored most biochemical markers. The oxidative disturbance due to AgNPs toxicity was obvious at the high dose of exposure. It is recommended that careful attention should be considered on the use of such molecules in sunscreens, cosmetics, pharmaceutical additives and food colorants and the use of natural matrices in synthesis of AgNPs. The most prominent pathological lesions observed in the liver were hepatocellular vacuolar degeneration and necrosis reported more cellular damage in the liver of mice exposed to AgNPs at a dose level of 20 mg/kg, in the form of swelling of cytoplasm, nuclear swelling, vacuole formation, abnormal hemorrhage, cellular congestion, and necrosis. These lesions were accompanied with elevation in serum ALT and AST.

Declarations

Conflict of interest

The authors declare that they have no competing interests.

Funding declaration

National Research Centre in Egypt with registration **No. 13 087**

Acknowledgement

The authors offer great thanks to the National Research Centre (NRC), Egypt for supporting and providing all necessary facilities to complete this research.

Author contributions

EMA, NSE, SAA and AMM participated in the whole design of this study; **SMG, SAA**, **NSE** and **WKB K** conducted the experiments and analyzed the data. All authors edited and revised the whole manuscript, read and approved the final version of the manuscript.

References

1. Yang L, Kuang H, Zhang W, Aguilar ZP, Wei H, Xu H (2017) Comparisons of the biodistribution and toxicological examinations after repeated intravenous administration of silver and gold nanoparticles in mice. Scientific Reports 7(1): 3303.
2. Abdel-Fattah WI, Ali GW (2018) On the anti-cancer activities of silver nanoparticles. Journal of applied biotechnology and bioengineering 5(2): 1–4.
3. Bao H, Yu X, Xu C, Li X, Li Z, Wei D, Liu Y (2015) New toxicity mechanism of silver nanoparticles: promoting apoptosis and inhibiting proliferation. PLoS One 10(3): e0122535.
4. Marassi V, Di Cristo L, Smith SGJ, Ortelli S, Blosi M, Costa AL, Reschiglian P, Volkov Y, Prina-Mello A 2018 Silver nanoparticles as a medical device in healthcare settings: a five-step approach for candidate screening of coating agents. Royal Society Open Science 5(1): 171113.
5. Mao BH, Chen ZY, Wang YJ, Yan SJ (2018) Silver nanoparticles have lethal and sublethal adverse effects on development and longevity by inducing ROS-mediated stress responses. Scientific Reports 8(1): 2445.
6. Ribeiro MJ, Maria VL, Scott-Fordsmand JJ, Amorim MJ (2015) Oxidative Stress Mechanisms Caused by Ag Nanoparticles (NM300K) are Different from Those of $AgNO_3$: Effects in the Soil Invertebrate Enchytraeus Crypticus. Int J Environ Res Public Health 12(8): 9589–602.
7. Granbohm H, Larismaa J, Ali S, Johansson LS Hannula SP (2018) Control of the Size of Silver Nanoparticles and Release of Silver in Heat Treated SiO-Ag Composite Powders. Materials (Basel) 11(1): 80.
8. Honary S, Ghajar K, Khazaeli P, Shalchian P (2011) Preparation, characterization and antibacterial properties of silver-chitosan nanocomposites using different molecular weight grades of chitosan. Tropical Journal of Pharmaceutical Research 10(1): 69–74.

9. Hu Z, Zhang D-Y, Lu S-T, Li P-W, Li S-D (2018) Chitosan-based composite materials for prospective hemostatic applications. Mar Drugs 16 (8): 273.
10. Lee, P. C., Meisel, D. Adsorption and surface – enhanced Raman of dyes on silver and gold sols. Journal of Physical Chemistry 1982; 86: 3391–3395.
11. Fernández-Urrusuno R, Calvo P, Remuñán-López C, VilaJato JL, Alonso MJ (1999) Enhancement of nasal absorption of insulin using chitosan nanoparticles. Pharmaceutical Research 16: 1576–1581.
12. Grenha A, Seijo B, Remunan-Lopez C (2005) Microencapsulated chitosan nanoparticles for lung protein delivery. European Journal of Pharmaceutical Sciences 25: 427 – 437.
13. Kim JS, Song KS, Sung JH, Ryu HR, Choi BG, Cho HS, Lee JK, Yu IJ (2013) Genotoxicity, acute oral and dermal toxicity, eye and dermal irritation and corrosion and skin sensitization of silver nanoparticles. Nanotoxicology 7(5): 953–60.
14. Ohkawa H, Ohishi N, Yagi K (1979) Assay of lipid peroxidation in animal tissue by thiobarbutyric acid reaction. Analytical Biochemistry 95: 351–358.
15. Bradford MM (1976) A rapid and sensitive method for the quantitation of microgram quantities of protein utilizing the principle of protein-dye binding. Anal Biochem 72: 248–254.
16. Montgomery HAC, Dymock JF (1961) The determination of nitrate in water. Analyst 86:414–416.
17. Beutler E, Duron O, Kelly B.M (1963) Improved Method for the Determination of Blood Glutathione. Journal of Laboratory and Clinical Medicine 61: 882–888.
18. Nishikimi M, Roa NA, Yogi K (1972) The occurrence of superoxide anion in the reaction of reduced phenazine methosulfate and molecular oxygen. Biochemical and Biophysical Research Communications 46: 849–854.
19. Rietman S, Frankle SA (1957) colorimetric method for determination of serum glutamic oxaloacetic and glutamic pyruvic transaminases. Am. J. Clin. Path 28: 56–63.
20. Babson AL, Greely SJ, Coleman CM, Philips GE (1966) Phenolphthalein monophosphate as a substrate for serum alkaline phosphatase. Clin. Chem 12: 482–490.
21. Szasz G (1969) A kinetic photometric method for serum gamma- glutamyl transpeptidase. Clin. Chem 15: 124–136.
22. El-Houseini ME, Mohammed MS, Elshemey WM, Hussein TD, Desouky OS, Elsayed AA (2005) Enhanced detection of hepatocellular carcinoma. Cancer Control 12(4): 248–53.
23. Marsh WJ, Fingerhut B, Miller H (1965) Automated and manual direct methods for the determination of blood urea. Clin Chem 11: 624–627.
24. Tracey KJ, Cerami A (1993) Tumor necrosis factor, other cytokines and disease. Annual Review of Cell Biology 9: 317–343.
25. Al-Rasheed NM, Faddah LM, Mohamed AM, Abdel Baky NA, Al-Rasheed NM, Mohammad RA (2013) Potential impact of quercetin and idebenone against immuno- inflammatory and oxidative renal damage induced in rats by titanium dioxide nanoparticles toxicity. Journal of oleo science 62(11): 961–971.

26. Fairbairn DW, Olive PL, O'Neill KL (1995) The comet assay: A comprehensive review. Mutat Res. 339(1): 37–59.
27. Blasiak J, Arabski M, Krupa R, Worzniak K, Zadrozny M, Kasznicki J, Zurawaska M and Drzewoski JJ (2004) DNA damage and repair in type 2 diabetes mellitus. Mutation Research. 554: 297–304.
28. Rosario F, Hoet P, Santos C, Oliveira H (2016) Death and cell cycle progression are differently conditioned by the AgNP size in osteoblast-like cells. Toxicology 368–369: 103–15.
29. Hirsch C, Zouain CS, Alves JB, Goes A (1997) Induction of protective immunity and modulation of granulomatous hypersensitivity in mice using PIII, an anionic fraction of *Schistosoma mansoni* adult worm. Parasitology 115: 21–28.
30. Tsiola A, Pitta P, Callol AJ, Kagiorgi M, Kalantzi I, Mylona K, Santi I, Toncelli C, Pergantis S and Tsapakis M 2017 The impact of silver nanoparticles on marine plankton dynamics: Dependence on coating, size and concentration. Sci Total Environ 601–602: 1838–48.
31. Kettler K, Giannakou C, de Jong WH, Hendriks AJ, Krystek P (2016) Uptake of silver nanoparticles by monocytic THP-1 cells depends on particle size and presence of serum proteins. J Nanopart Res 18(9): 286.
32. Wen H, Dan M, Yang Y, Lyu J, Shao A, Cheng X, Chen L, Xu L (2017) Acute toxicity and genotoxicity of silver nanoparticle in rats. PLoS One 12(9): e0185554.
33. Li S, Tan H-Y, Wang N, Zhang Z-J, Lao L, Wong C-W, Feng Y (2015) The Role of Oxidative Stress and Antioxidants in Liver Diseases. Int. J. Mol. Sci 16: 26087–26124.
34. Glinski A, Liebel S, Pelletier È, Voigt CL, Randi MAF, Campos SX, Ribeiro CAO and Neto FF (2016) Toxicological interactions of silver nanoparticles and organochlorine pesticides in mouse peritoneal macrophages. Toxicology Mechanisms and Methods 26(4), 251-259.
35. Adeyemi OS, Faniyan TO (2014) Antioxidant status of rats administered silver nanoparticles orally. Journal of Taibah University Medical Sciences 9(3): 182–186.
36. Alarifi S, Ali D, Al Gurabi MA, Alkahtani S (2016) Determination of nephrotoxicity and genotoxic potential of silver nanoparticles in Swiss albino mice. Toxicological & Environmental Chemistry 99(2): 294–301.
37. Żuberek M, Paciorek P, Bartosz G, Grzelak A (2017) Silver nanoparticles can attenuate nitrative stress. Redox Biol 11: 646–652.
38. Ngo DH and Kim SK (2014) Antioxidant effects of chitin, chitosan, and their derivatives. Adv Food Nutr Res 73: 15–31.
39. Rizk MZ, Ali SA, Hamed MA, Saba El-Rigal N, Aly HF, Salah HH (2017) Toxicity of titanium dioxide nanoparticles: Effect of dose and time on biochemical disturbance, oxidative stress and genotoxicity in mice. Biomedicine & Pharmacotherapy 90: 466–472.
40. Monfared AL, Soltani S 2013 Effects of silver nanoparticles administration on the liver of rainbow trout (Oncorhynchus mykiss): histological and biochemical studies. European Journal of Experimental Biology 3(2):285–289.

41. Franzini M, Pompella A, Corti A (2014) Gamma-glutamyltransferases: exploring the complexity of a multi-functional family of enzymes. Front Pharmacol 5(221): 1–2.
42. Udristioiu A, Iliescu RG, Cojocaru M, Joanta A (2014) Alkaline phosphatase isoenzymes and leukocyte alkaline phosphatase score in patients with acute and chronic disease: a brief review. British journal of medicine & medical research 4(1): 340–350.
43. Parivar K, Fard FM, Bayat M, Alavian SM (2016) Motavaf M. Evaluation of iron oxide nanoparticles toxicity on liver cells of balb/c rats. Iran Red Crescent Med J 18(1): e28939.
44. Shati AA, Elsaid FG and Hafez EE (2011) Biochemical and molecular aspects of aluminium chloride-induced neurotoxicity in mice and the protective role of crocus sativus L. extraction and honey syrup. Neuroscience 175: 66–74.
45. Chien R-C, Yen M-T, Mau J-L (2016) Antimicrobial and antitumor activities of chitosan from shiitake stipes, compared to commercial chitosan from crab shells. Carbohydrate Polymers 138: 259–264.
46. Khanna P, Ong C, Bay BH, Baeg GH (2015) Nanotoxicity: Interplay of Oxidative Stress, Inflammation and Cell Death. Nanomaterials 5: 1163–1180
47. Shrivastava R, Kushwaha P, Bhutia YC, Flora S (2016) Oxidative stress induced following exposure to silver and gold nanoparticles in mice. Toxicology and Industrial Health 32(8): 1391–1404.
48. Bastos V, Duarte IF, Santos C, Oliveira H (2017) Genotoxicity of citrate-coated silver nanoparticles to human keratinocytes assessed by the comet assay and cytokinesis blocked micronucleus assay. Environ Sci Pollut Res Int. 24(5):5039–5048.
49. Lebedová J, Hedberg YS, Wallinder IO, Karlsson HL (2018) Size-dependent genotoxicity of silver, gold and platinum nanoparticles studied using the mini-gel comet assay and micronucleus scoring with flow cytometry. Mutagenesis 33(1): 77–85.
50. Jagani HV, Josyula VR, Palanimuthu VR, Hariharapura RC, Gang SS (2013) Improvement of therapeutic efficacy of References 199 PLGA nanoformulation of siRNA targeting anti-apoptotic Bcl-2 through chitosan coating. Eur J Pharm Sci. 48(4–5): 611–8.
51. Fatemi M, Moshtaghian J, Ghaedi K, dinani NJ and Naderi G (2017) Effects of silver nanoparticle on the developing liver of rat pups after maternal exposure. Iranian Journal of Pharmaceutical Research 16(2):685–693.
52. Dănilă OO, Berghian AS, Dionisie V, Gheban D, Olteanu D, Tabaran F, Baldea I, Katona G, Moldovan B, Clichici S, David L, Filip GA (2017) The effects of silver nanoparticles on behavior, apoptosis and nitro-oxidative stress in offspring Wistar rats. Nanomedicine 12(12): 1–19.
53. Ali SA, Arafa AF, Aly HF, Ibrahim NA, Kadry MO, Abdel-Megeed RM, Hamed MA, Farghaly AA, El Regal NS, Fouad GI, Khalil WKB, Refaat EA (2020) DNA damage and genetic aberration induced via different sized silver nanoparticles: Therapeutic approaches of *Casimiroa edulis* and *Glycosmis pentaphylla* leaves extracts. J Food Biochem e13398: 1–14
54. Hassanen E I, Khalaf AA, Tohamy AF, Mohammed ER, Farroh KY (2019) Toxicopathological and immunological studies on different concentrations of chitosan-coated silver nanoparticles in rats International Journal of Nanomedicine 14:4723–4739

Figures

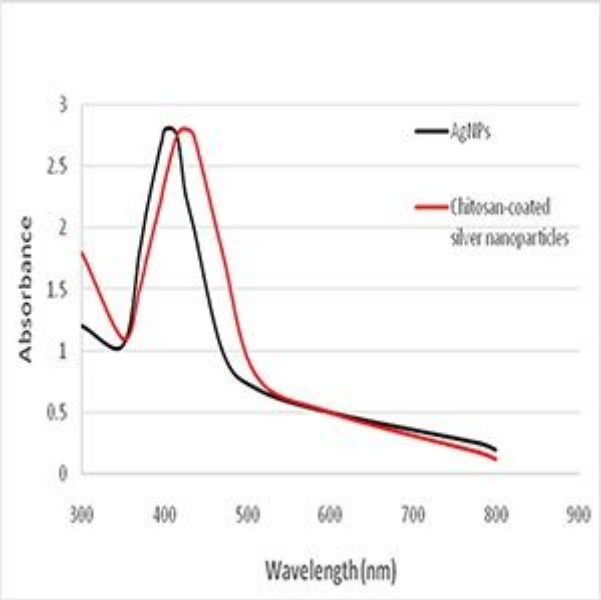

Figure 1

UV–Vis absorption spectra of 25±5 nm particle size of AgNPs and chitosan- coated silver nanoparticles

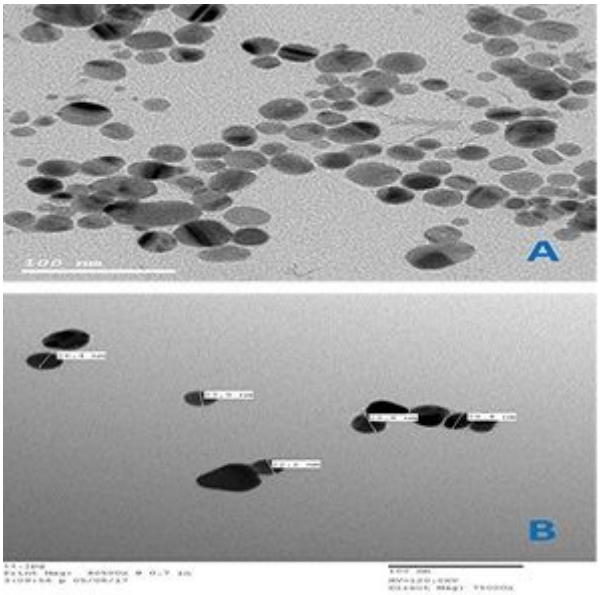

Figure 2

Transmission electron microscope images (TEM) of25±5 nm AgNPs (A) and chitosan- coated AgNPs (B).

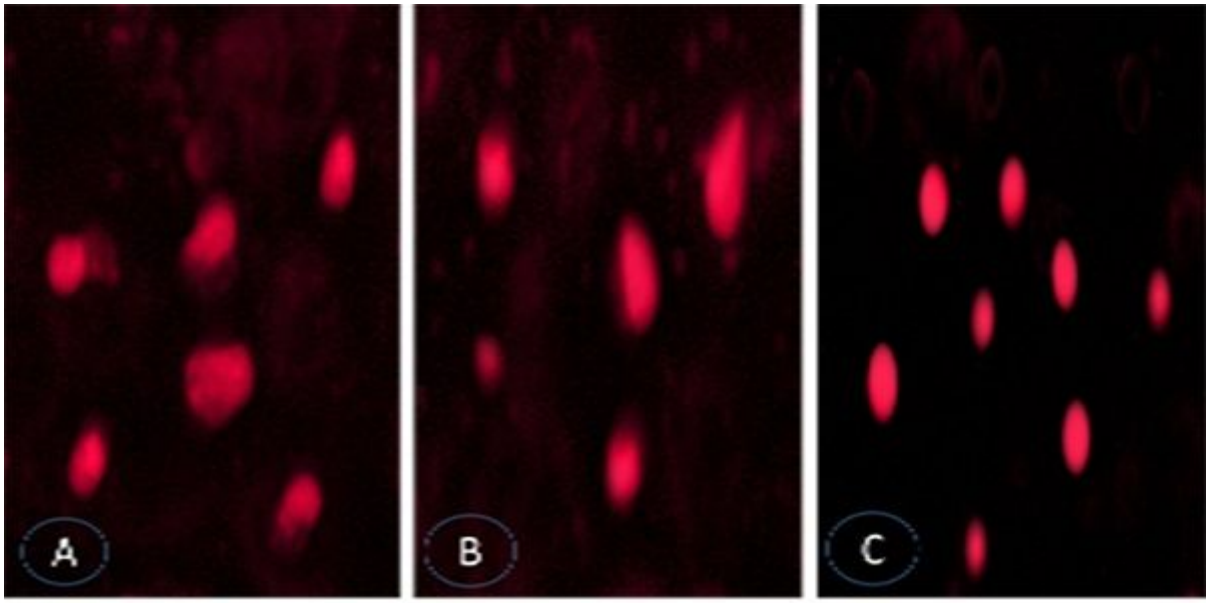

Figure 3

Visual score of DNA damage [A] (classes 1, 2 and 3); [B] (classes 2 and 3) and [C] (class 0a) using comet assay in liver samples exposed to AgNPs and chitosan- coated AgNPs.

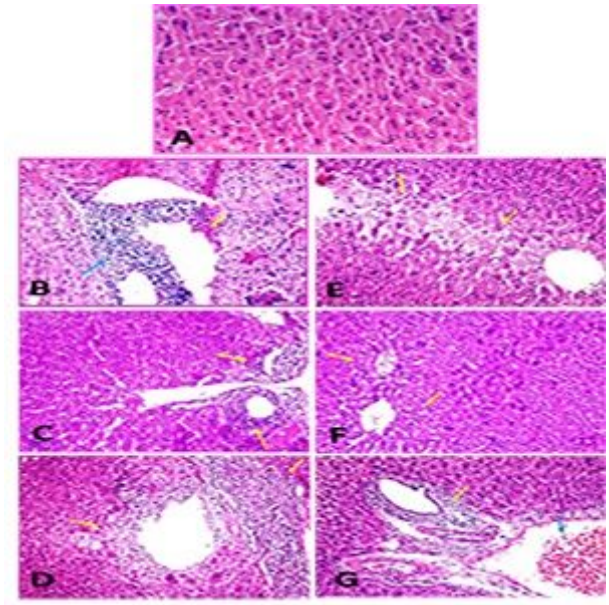

Figure 4

Photomicrograph of liver sections of mice (H & E x200).Normal hepatocytes in control tissues (A);AgNPs 25±5 nm, 25mg/kg (B); 50mg/kg (C); 100mg/kg (D); Ch-AgNPs 25±5 nm, 25mg/kg (E); 50mg/kg (F); 100mg/kg (G).

Supplementary Files

This is a list of supplementary files associated with this preprint. Click to download.

- GraphicalAbstract..tif